Molecular Systems Biology 4; Article number 181; doi:10.1038/msb.2008.20
Citation: ***Molecular Systems Biology*** **4:181**

www.molecularsystemsbiology.com

molecular systems biology

REPORT

Synthetic gene brushes: a structure–function relationship

Amnon Buxboim[1], Shirley S Daube[2] and Roy Bar-Ziv[1,*]

[1] Department of Materials and Interfaces, The Weizmann Institute of Science, Rehovot, Israel and [2] Chemical Research Support Unit, The Weizmann Institute of Science, Rehovot, Israel
* Corresponding author. Department of Materials and Interfaces, The Weizmann Institute of Science, Herzel Street, Rehovot 76100, Israel.
Tel.: +972 8 9342069; Fax: 972 8 9344138; E-mail: roy.bar-ziv@weizmann.ac.il

Received 29.10.07; accepted 25.2.08

We present the assembly of gene brushes by means of a photolithographic approach that allows us to control the density of end-immobilized linear double-stranded DNA polymers coding for entire genes. For 2 kbp DNAs, the mean distance varies from 300 nm, where DNAs are dilute and assume relaxed conformations, down to 30 nm, where steric repulsion at dense packing forces stretching out. We investigated the gene-to-protein relationship of *firefly luciferase* under the T7/*E.Coli*-extract expression system, as well as transcription-only reactions with T7 RNA polymerase, and found both systems to be highly sensitive to brush density, conformation, and orientation. A 'structure–function' picture emerges in which extension of genes induced by moderate packing exposes coding sequences and improves their interaction with the transcription/translation machinery. However, tighter packing impairs the penetration of the machinery into the brush. The response of expression to two-dimensional gene crowding at the nanoscale identifies gene brushes as basic controllable units *en route* to multicomponent synthetic systems. In turn, these brushes could deepen our understanding of biochemical reactions taking place under confinement and molecular crowding in living cells.

Molecular Systems Biology 15 April 2008; doi:10.1038/msb.2008.20
Subject Categories: synthetic biology
Keywords: in vitro synthetic biology; nano-biotechnology; cell-free gene expression; molecular crowding; biochip

Introduction

Synthetic biological systems *in vitro* have recently attracted attention, holding promise as model systems for reducing biological complexity and for the development of new hybrid functional materials (see recent review by Forster and Church, 2006; Doktycz and Simpson, 2007). *In vitro* transcription could be used to design DNA-based devices and switches (Dittmer and Simmel, 2004; Dittmer *et al*, 2005; Kim *et al*, 2006), and to produce RNA molecules with regulatory and catalytic capabilities (Isaacs *et al*, 2006) that could ultimately interface with nanoscale DNA nanomechanical systems (reviewed by Seeman, 2005). Incorporating the complete transcription/translation reaction expands the scope of *in vitro* synthetic systems, for example to evolve novel proteins (Tawfik and Griffiths, 1998; Seelig and Szostak, 2007), synthesize protein nano-assemblies (Daube *et al*, 2007), explore synthetic gene circuits (Noireaux *et al*, 2003; Ishikawa *et al*, 2004; Isalan *et al*, 2005), and eventually develop artificial cells (Shimizu *et al*, 2001; Noireaux and Libchaber, 2004; Noireaux *et al*, 2005; Forster and Church, 2006; Luisi *et al*, 2006; Sunami *et al*, 2006; Murtas *et al*, 2007). Synthetic systems based on cell-free gene expression would benefit from appropriate materials platforms, and a surface with immobilized genes is an innate platform to regulate biosynthetic reactions (Shivashankar *et al*, 2000), separate them spatially, and cascade their action by diffusion (Buxboim *et al*, 2007). On a surface, we can explore primitive forms of regulation, as compared with those used in living cells and ones who rely on physical constraints, geometry, and symmetry breaking, which would be difficult to implement in bulk solution or inside a lipid vesicle (Tawfik and Griffiths, 1998; Szostak *et al*, 2001; Noireaux and Libchaber, 2004; Forster and Church, 2006; Sunami *et al*, 2006; Murtas *et al*, 2007). However, progress has been so far hindered by our

inability to control the immobilization of genes on a surface and to efficiently express them. Here, we used a unique biochip platform (Buxboim *et al*, 2007) to introduce dense gene brushes as a very primitive emulation of the cell nucleus.

Inert polymer brushes are abundant and useful in everyday complex fluid systems and we recall their basic feature (Milner, 1991). Consider linear polymers attached to a surface. Their first tendency is to form short brushes with random-walk configurations in order to maximize the entropy. A second one is to form sparse tall brushes in order to be wet by solvent. These tendencies contradict if the distance between attachment sites is much smaller than the polymer radius of gyration. Hence the polymer free energy is a balance of two costs, namely stretching, which reduces their entropy, and overlapping with neighboring chains, which reduces the favorable contact with the solvent (Milner, 1991). As a result, at tight packing, the polymers adopt a configuration that is extended beyond their solution end-to-end distance.

The assemblies presented here are made of end-attached linear double-stranded DNA (dsDNA) polymers coding for entire genes, whose lengths are a few thousand base pairs (bp) with controlled densities, ranging from sparse configurations to dense ones, with a local DNA concentration similar to that of *Escherichia coli*. An unexplored area in materials science, these synthetic gene brushes open the possibility to encode a biochemical function into the material: the physical properties of the brush may affect the biochemistry of biosynthetic reactions, and gene products could, in turn, change brush properties. Here, the first part of this possible feedback loop is explored by a 'structure–function' study that seeks to unravel the affect of two-dimensional gene crowding on biosynthetic reactions.

We recently observed a nonlinear relationship between proteins expressed from immobilized genes in a T7 RNA polymerase (RNAP)/wheat-germ extract, where prokaryotic transcription is *a priori* uncoupled from the eukaryotic translation machinery (Buxboim *et al*, 2007). This initial observation, lacking the most natural comparison between gene expression on a surface and that in solution, had stimulated a more rigorous search for an underlying mechanism of the pattern observed. For a basic understanding of the effect of gene localization on expression, it is imperative to identify the machinery components most sensitive to DNA surface configuration. It is important to elucidate the interplay between surface transcription and the concomitant translation, which can occur either from nascent transcripts or from fully released ones, depending on the particular expression system used and on the biophysical constraints on the surface. Here, we assembled gene brushes encoding for *firefly luciferase* reporter under control of the T7 promoter (*T7-luc* construct) and then carried out coupled transcription/translation in *E. coli* cell extracts as well as T7 transcription in a buffer on surfaces as a function of the brush density, conformation, and orientation, and in comparison with solution. We found that protein synthesis is significantly affected by gene brush structure, exhibiting simple linear gene-to-protein relationship for stretched genes and nonlinear, sigmoidal behavior for dilute relaxed conformations. We observed attenuation at dense gene packing only in the transcription/translation reactions and not in the transcription-only reactions, most likely due to molecular crowding and sensitivity of the translation machinery to the orientation of the grafted genes. The transcription-only assays imply that RNAP is indeed the primary sensor of brush properties. Biosynthetic kinetics and lifetime measurements allow us to deduce a significant enrichment of product accumulation near the surface and their spatial gradients.

Results and discussion

Gene brush assembly

We used a biochip platform for cell-free gene expression based on a new single-step photolithographic biocompatible monolayer (Buxboim *et al*, 2007) (termed 'daisy'). A daisy molecule is comprised of a polyethyleneglycol backbone with a silicon-binding group at one end and an amine-protecting group at the other (Buxboim *et al*, 2007). Daisy molecules readily coat silicon dioxide, forming a smooth monolayer with amines every $\sim 1.6 \times 1.6\,\mathrm{nm}^2$ that become available for chemical binding upon UV irradiation of the surface. Following photo deprotection of amines, we chemically bind biotin and then immobilize streptavidin-conjugated linear dsDNAs (SA-DNA) on the surface-bound biotins. The spatial pattern of dsDNAs on the surface can be determined by projecting a photo-mask: flux-dependent partial deprotection of amines through the mask converts image grayscale into surface density, as shown, for example, in Figure 1A. The dsDNA brush is maintained in an aqueous solution to avoid collapse of the structure. Thus, by controlling the UV flux, we can prepare brushes with spatially varying surface densities. We verify the process of dsDNA photolithography by labeling dsDNA independently both at its surface proximal (green) and solution distal (red) ends (Figure 1A).

For studying the characteristics of protein biosynthesis as a function of gene density, we developed a quantitative DNA grafting assay that would allow us to more accurately quantify the density of grafted DNA. In this assay, rather than varying the UV flux (Buxboim *et al*, 2007) (Figure 1A), we exposed daisy-coated chips uniformly (without a mask) and at the maximal UV flux required for deprotection of all surface amines. Following binding of biotin to the exposed amines, SA-DNAs at variable solution concentrations were incubated for attachment on the surfaces, which were then extensively washed. To accurately evaluate the correlation between solution concentration and equilibrium DNA surface density, we used radioactively-labeled dsDNAs, 420, 2160, and 2900 bp long with contour lengths of 140, 720, 960 nm, and an estimated relaxed end-to-end distance of 85, 240, 295 nm, respectively (Valle *et al*, 2005) (Figure 1B). The two long dsDNAs are composed of several persistence lengths (l_p=44 nm; Valle *et al*, 2005), whereas the short DNA fragment consists of a maximum of two persistence lengths. The mean distances between dsDNAs at equilibrium, for the three lengths, decreased monotonously with their solution concentrations, from 150, 235, 250 nm at dilute surfaces to 15, 30, 36 nm at maximal packing (Figure 1B). Correspondingly, the maximal density of dsDNAs on the surface was 4000, 1070, 735 dsDNAs per μm^2.

A direct measurement of brush height and structure is experimentally challenging and beyond the scope of this work.

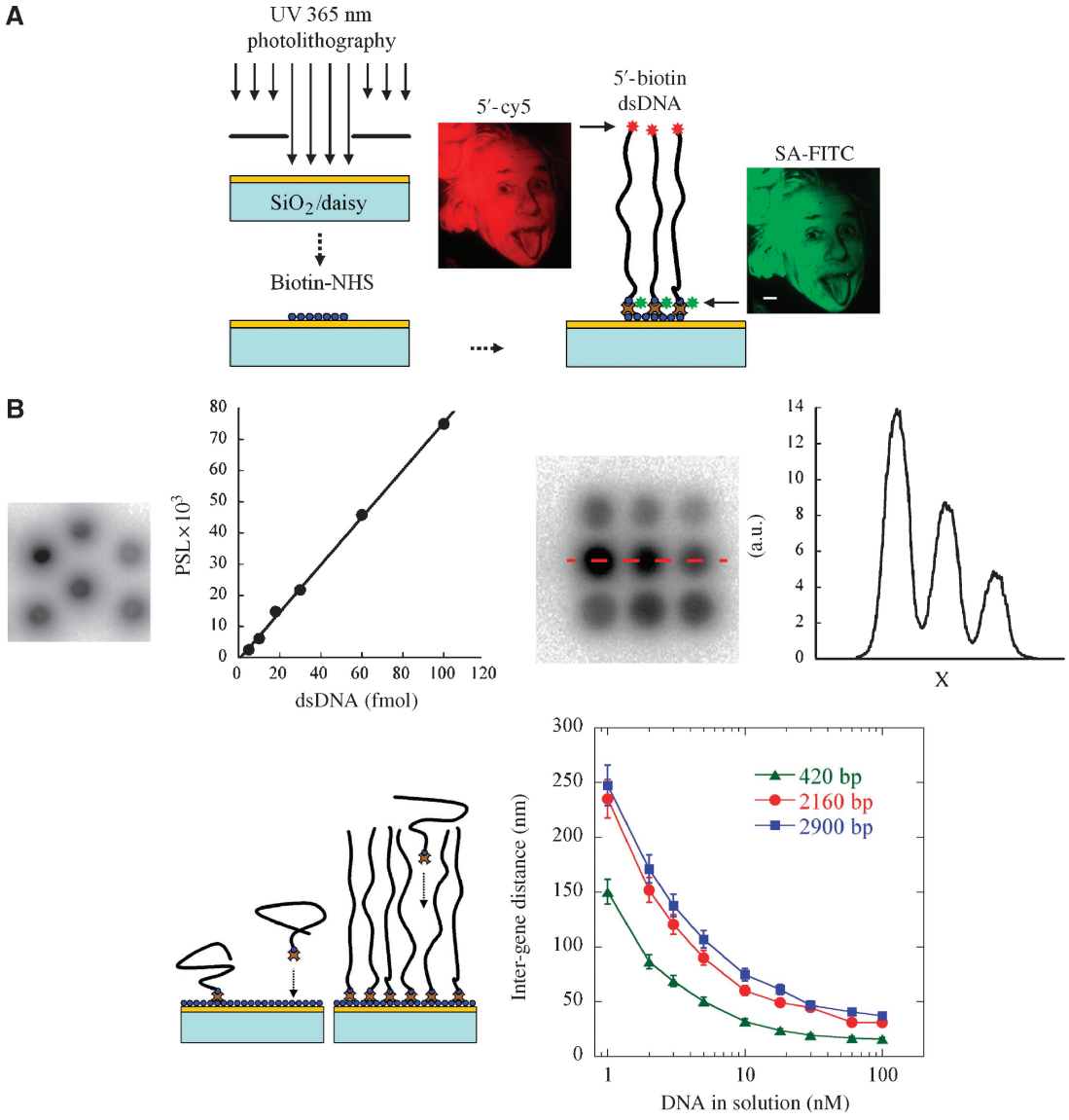

Figure 1 (**A**) Daisy biochip platform. Daisy molecules form a photolithographic monolayer (yellow) on silicon dioxide (light blue) in a single step. Following UV light photo-deprotection through an image mask, we bind biotin (blue circles) to free amines via NHS (Supplementary information). Streptavidin-conjugated dsDNA (SA-DNA, brown) are then immobilized with the mask grayscale translated into surface density of dsDNA imaged by dual fluorescent tags, FITC (green) covalently attached to the SA, and cy5 (red) covalently attached to the DNA at its surface-distal end. Scale bar is 50 μm. (**B**) Assembly of uniform linear dsDNA brushes. The packing of linear dsDNA polymer brushes following uniform deprotection of daisy-coated chips was quantified by radioactive labeling (Supplementary information) of 420 (green), 2160 (red), and 2900 (blue) bp DNA. Each radioactive spot in a 3 × 3 array contained a different amount of DNA (shown above the graph) as imaged by phosphorimaging densitometry (Methods and materials). The signal from the adsorbed DNA was converted to number of molecules using a calibration curve deduced from spots of known amounts of radioactive DNA on the surface (left). The equilibrium mean distance between dsDNAs was dictated by their solution concentration (main plot).

Nonetheless, we note the following: (a) SA-DNA binds specifically to the surface through the SA–biotin bond, rather than nonspecifically at multiple points along the DNA polymer. This is evident from control experiments where we achieved specific end-attachment ratios of 50–200 as measured with respect to SA-DNA adsorbed to unexposed daisy surfaces, or to DNA not conjugated to SA that were adsorbed to fully exposed daisy surfaces. Realizing that the DNAs are specifically end-anchored to the surface and that they pack maximally at distances that are smaller than the persistence length, the rest of the polymer must extend out into solution to minimize its free energy (Milner, 1991). (b) The assembly of dsDNAs on the surface slows down considerably after a few hours (data not shown) supporting the notion that a tightly packed DNA arrangement had been formed on the surface, hampering the ability of additional SA-DNA from reaching the surface. Altogether, our brush density data necessarily supports a picture in which the dsDNAs at high density must acquire an extended conformation. This interpretation does not necessarily invoke complete extension of the DNA polymer chain, but rather a more extended conformation than the mushroom-like relaxed conformation, resulting in a brush

height that is larger than the dsDNA's end-to-end distance. Therefore, the DNA brush schemes in the remaining of the figures are intended as a qualitative guide to depict the change in DNA conformation upon increase in density. The structure of these gene brushes is most likely intermediate between long flexible polymers and rod-like molecules.

Sigmoidal response of protein expression from surface-bound genes

We studied the effect of gene localization on expression by immobilizing the *T7-luc* construct on surfaces followed by bathing the surfaces with an *in vitro* transcription/translation reaction mix. The T7 promoter was oriented close to the surface, separated by a 60 bp spacer (~20 nm), with synthesis of mRNA directed outward into the solution (Figure 2A). The aqueous solution was at a height of about 1.5 mm above the chip in an open reaction chamber that allowed us to collect aliquots of luciferase expressed on the surface and released into solution after a few hours of reaction. For comparison, we expressed luciferase from genes in solution, while maintaining the *same* gene number (in moles) and reaction volume as on the surface (Figure 2A). The data showed the following features: (a) expression in solution followed a simple gene/protein linear relationship, whereas on a chip, the curve was nonlinear with a power law of 2.5 ± 0.5; (b) the expression attenuated at high gene number on the chip; (c) saturation of expression on the chip occurred at 30-fold fewer genes than in solution.

Orientation of surface-bound genes affects expression

The marked differences between biosynthesis on the surface and in solution, done at identical conditions except for gene localization, hint that brush structure is important for the expression efficiency of genes. Guided by the crowded nature of the brush, we searched for the origin of these distinct characteristics in the orientation of the genes with respect to the surface, reasoning that (a) if the surface-bound DNAs do not form a brush, then no effect of promoter orientation and distance would occur, and (b) if DNA brush does forms, then placing the promoter at the top of the brush rather than at the bottom may improve its accessibility to the machinery. To test these hypotheses, we assembled gene brushes once with their streptavidin conjugated at the promoter proximal end, and alternatively at the promoter distal end, resulting in 'bottom' and 'top' configurations, respectively (Figure 2B). We carried out the same *firefly luciferase* expression experiment from 'bottom' and 'top' at varying gene number. Indeed, we found that top-oriented genes yielded a significant increase in the expression compared with bottom-oriented ones for the entire gene number range (Figure 2B). This result is consistent with experiments done with DNA immobilized on beads (Nord *et al*, 2003) and provide strong evidence to support DNA extension at high gene densities.

A structure–function relationship of protein expression from gene brushes

The details of DNA brush build up (Figure 1B) have strongly implied, concomitantly with an increase in gene density, a gradual change of dsDNA structure, from a sparse and relaxed conformation to an extended dense brush. To isolate the effect of dsDNA structure on expression, we therefore varied the gene number while fixing the overall dsDNA density to the highest value. This was achieved by adding 'dummy DNA' of equal length to the genes but without promoter and coding regions. We prepared nine dsDNA brushes with equal overall dsDNA (gene and dummy), but each with a different ratio of bottom-oriented genes to dummy DNA. Hence, for all gene and dummy combinations, the total amount of DNA applied on the surface was identical, resulting in a similar conformation of the dsDNA (Figure 2, scheme). The expression of luciferase from the mixed gene/dummy brushes showed a simple linear gene/protein relationship, in contrast to the sigmoidal behavior observed in the gene-only brushes (Figure 2C). As expected, the gene-only and gene/dummy curves merged at maximal gene number where their content is basically identical and composed only of genes.

We verified that dummy DNA did not affect transcription/translation efficiency in solution (not shown) and we hence postulate that its significant effect on expression from the surface is due to its modulation of DNA structure. Further insight is gained by replotting the utility of the genes (Figure 2D), defined by the number of proteins synthesized divided by the number of genes, as a function of the mean intergene distance derived from the dsDNA surface densities (Figure 1), rather than total expression as a function of gene number (Figure 2C). The utility of genes in the gene/dummy systems is essentially constant, independent of distance. The crossover points between the gene-only and gene/dummy plots identified three gene-number regimes (Figure 2, I, II, III): at low gene densities (regime I), where the mean distance

Figure 2 (**A**) Protein biosynthesis on a chip and in solution. Transcription/translation of *luciferase* using the T7/*E. Coli*-extract system in solution and on the chip with identical number of genes and reaction volume; the arrows indicate the position and direction of the T7 promoter within the 2160-bp-long dsDNA. The total amount of luciferase synthesized after 3 h of incubation is plotted. (**B**) Expression from top- and bottom-oriented genes. Chips with varying amounts of DNA, and hence density, were prepared with genes oriented either with the promoter directed into the surface (top) or toward the solution (bottom) sides. The amount of luciferase synthesized as a function of gene number is plotted (Material and methods). (**C**) Effect of brush structure on expression. Transcription/translation on a chip from variable 'gene-only' (left bottom scheme) and fixed 'gene/dummy' density brushes (right bottom scheme). The 'gene/dummy' brushes were maximally packed at the highest density with varying ratio of gene-to-dummy DNA. The amount of expressed luciferase produced in a 10 μl reaction volume placed on top of a 7 mm^2 surface covered with DNA is plotted as a function of gene number. (**D**) Effect of brush structure on expression utility. Transcription/translation on a chip from variable 'gene-only' and fixed 'gene/dummy' density brushes. The expressed luciferase per gene is plotted as a function of mean intergene distance. (**E**) Transcription-only configuration in a buffer on a chip as a function of gene number for 'top' and 'bottom' orientations. (**F**) Transcription-only configuration in a buffer on a chip from variable 'gene-only' and fixed 'gene/dummy' density brushes.

between adjacent genes varies from 300 to 150 nm, the gene/dummy configuration was significantly more efficient than gene-only configuration. At the intermediate regime II (150–60 nm), the gene-only configuration became increasingly favorable as the intergene distance reached the 60 nm value. From that point onward (regime III; 60–30 nm), the expression

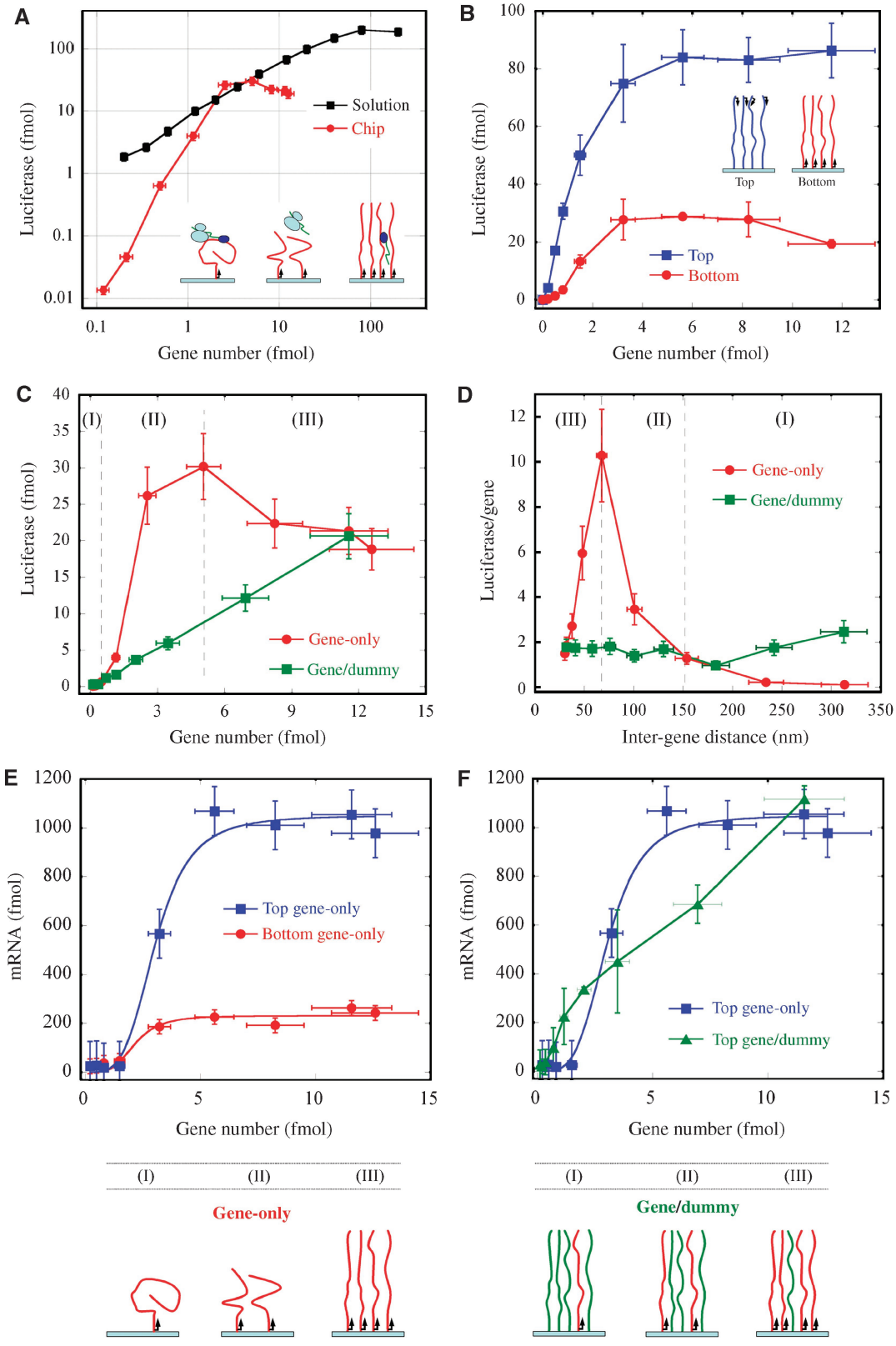

efficiency of the gene-only configuration attenuated to the constant value displayed by the gene/dummy system.

We hypothesized that, in the dilute regime, gene-only configuration assumes a relaxed, nonoverlapping conformation, which is less favorable for the machinery than extended genes (Figure 2C and D, regime I). Upon decreasing the distance from 300 to 150 nm (regime I), the genes begin to overlap and experience mutual steric repulsion and hence assume an extended conformation. It is well established that the height of long polymer brushes extends nonlinearly with polymer surface density (Milner, 1991). As dsDNAs extend, they are likely to be more accessible to the biochemical machinery than the 'solution-like' conformation in the dilute regime. In regime II, with intergene distances of 60–150 nm, the conformations of gene-only and those of genes/dummy are similarly stretched; yet, the actual density of dsDNA is higher in the latter. At high density, the machinery must be impeded from efficiently propagating down the brush, which is consistent with gene-only conformations being more efficient than those of genes/dummy in this regime. Indeed, in regime III, the densities of the two systems become progressively comparable as the intergene distance approaches the 30 nm limit and their expression efficiencies match. The 60 nm peak in expression marks a balance between the improvement due to extension at moderate density and the impediment due to crowding at high density. In contrast, the gene/dummy system has a fixed density and structure for the entire gene number range and hence the efficiency of expression per gene remains constant.

To elucidate the role played by T7 RNAP in sensing the properties of the brush, we carried out transcription-only assays in an optimized buffer, rather than in the extract, and repeated the gene-only and gene/dummy experiments (Figure 2E and F; Supplementary Figure S2). The salient features observed in protein synthesis were recapitulated in these transcription-only assays, suggesting that RNAP is the primary sensor of the DNA brush. Importantly and in contrast to transcription/translation, these transcription-only experiments did not show any attenuation at high gene number in any of the configurations tested, consistent with the notion that the attenuation observed in the transcription/translation (Figure 2C) is a manifestation of impediment of ribosome penetration into the brush at high densities.

We note that, in all experiments comparing 'top', 'bottom', and solution, the 'bottom' always saturated at lower values. This could possibly stem from nucleotide depletion within the brush. However, we disfavor this scenario, as nucleotide depletion should affect the rate of synthesis during the elongation step of transcription, which takes place along the entire length of the DNA. Therefore, any gradients of nucleotide concentrations are expected to alter RNA synthesis rates, whether initiating at the 'top' and terminating at the 'bottom' or vice versa. It is more likely that the initiation step of transcription, namely promoter binding, rather than the elongation step, should be affected by the localization of the promoter with respect to the surface. We therefore suggest that the marked differences between 'bottom' and 'top' configurations are due to changes in the local concentration of RNAP near the surface and at the interface with the solution, respectively. Although changes in salt concentrations may also affect binding of RNAP to the promoter, we suggest that salt gradients do not play a major role in determining transcription levels in the brush because of the following reasons: (a) the screening length is $\sim$2 nm under the experimental conditions; (b) the distance of the promoter from the surface is no less than 30 nm; (c) the distance between dense DNAs is also $\sim$30 nm.

Surface-induced enrichment of biosynthetic products and concentration gradients

The above analysis stemmed from a comparison between expression curves on the surface at different DNA densities, but neglected to account for the marked differences between expression in *solution* and on the surface (Figure 2A). We ruled out the possibility that these differences resulted from biochemical effects on the rates of translation per mRNA (Supplementary Figure S1, c) and we have also shown that translation could occur from freely diffusing mRNA, uncoupled from the transcription process (not shown). Therefore, to fully appreciate the difference between solution and surface expression, we must consider the spatial distribution of both transcription and translation in the solution surrounding the brush. Unlike the DNA, the mRNA and protein expressed on the chip are not physically immobilized. Yet, as we now show by a simple calculation, they must be confined to a thin diffuse layer next to the surface.

On the chip, mRNA molecules originate from the 'nucleus' of localized genes. Although they are free to diffuse, their escape from the surface is limited by mRNA degradation in the cell extract (Supplementary Figure S1). The transcription reaction can therefore be modeled as a one-dimensional reaction-diffusion equation with a localized source at z=0, combined with degradation. The steady-state solution is an exponential decaying concentration profile (Supplementary information):

$$R_{ss}(z) = \frac{\nu_{tx} \cdot \sigma \cdot \sqrt{\tau}}{\sqrt{D_{mRNA}}} e^{-z/\lambda}$$

where ν_{tx} is the transcription rate, σ=990 genes μm^{-2} is the gene density, τ=20 min is the mRNA lifetime, $D_{mRNA} \approx 6.5\,\mu m^2\,s^{-1}$ is its diffusion constant and $\lambda = \sqrt{D_{mRNA} \cdot \tau} = 90\mu m$ is the decay length (Figure 3A). Consequently, although the *total* mRNA synthesis on the chip was 1/2 than that in solution (Supplementary Figure S1, a), the *local* mRNA concentration in the vicinity of the surface was actually significantly higher relative to the corresponding solution expression by a factor $(\nu_{tx}^{chip}/\nu_{tx}^{sol})(L/\lambda) \approx 8$, where L=1.5 mm is the chamber height (Supplementary information). Given the same transcription rates and diffusion constant, faster degradation would lead to a sharper gradient.

Translation follows transcription not only from nascent mRNAs in the gene brush, but also from fully transcribed diffusing ones. Hence, the level of protein translation is proportional to the local mRNA concentration and to the translation rate. Unlike the mRNA, luciferase is not degraded in the cell extract and hence its synthesis cannot reach a steady-state concentration profile (this may not be the case for other proteins). Therefore, we solved for the time-dependent accumulation of luciferase from the brush (Supplementary

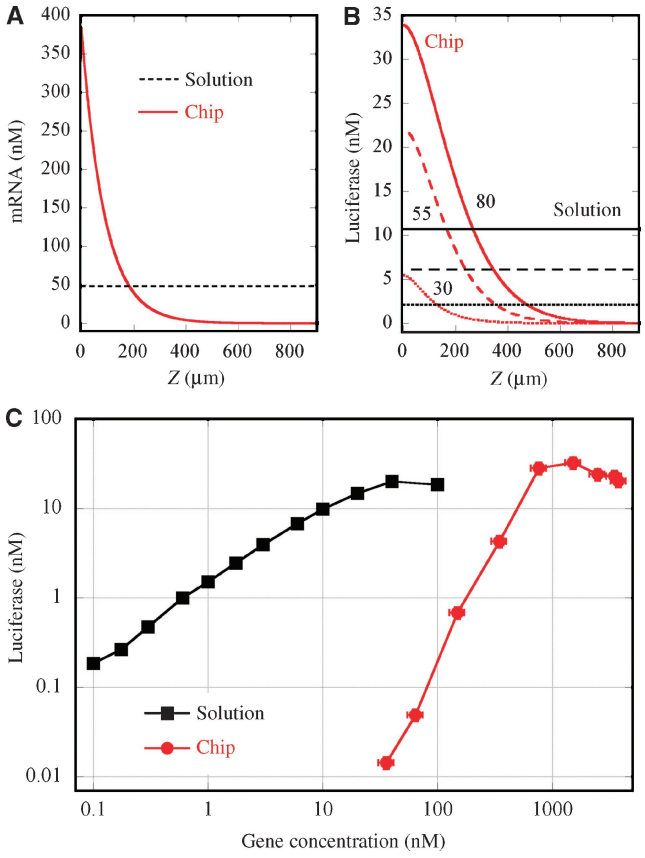

Figure 3 mRNA and luciferase synthesis spatial profiles. The mRNA spatial profile (**A**) away from the brush (at z=0) relative to synthesis in solution (chip, red; solution, dashed black) was computed based on rate equations (Supplementary information) and the measured transcription and translation rates. (**B**) The luciferase profile does not reach steady state and is shown for t=30, 55, and 80 min, relative to solution (chip, red; solution, black). (**C**) Replotting Figure 2A after rescaling gene and protein numbers by brush and diffuse layer heights, h_{brush}=500 nm and h_{luc}=140 μm.

information). At short times, the profile of protein concentration follows the mRNA exponential profile confined within 90 μm from the surface (Figure 3B). With time, protein diffusion becomes significant and the protein profile resembles a Gaussian distribution centered at z=0 with a typical width of $\sqrt{D_{luc} \cdot t}$. After t=2τ, most of the luciferase in our on-chip expression reaction would be found concentrated at a layer of h_{luc}=140 μm above the DNA brush and, as in the case of mRNA, its local concentration is higher than the solution expression experiment.

The analysis of mRNA and protein concentration gradients points to a more realistic comparison between solution and surface expression, by taking into account the localization of genes and their protein products and rescaling their gene and protein numbers (Figure 2A) to *effective concentration* according to the ratios of L/h_{brush} and L/h_{luc}, respectively, with $h_{brush} \approx 500$ nm (Figure 3C). Presenting the expression profile of solution and chip each in their own corresponding effective volumes provides a new perception of on-chip expression, one that is highly efficient and localized compared with solution.

Summary

The above analysis presents, in our view, the hallmark of expression from gene brushes: a heterogeneous system with localized, highly concentrated, and oriented DNA molecules, immersed in a solution of freely diffusing protein machinery. Protein biosynthesis is highly sensitive to gene density, conformation, and orientation. Gene expression products are localized in the vicinity of the brush due to the interplay of degradation, synthesis, and diffusion rates. Gene brushes could be used to deepen our understanding of other DNA-based reactions where confinement and crowding are expected to play a role, such as recombination, restriction, and methylation. In turn, fundamental understanding of gene brushes could be used to develop new synthetic systems based on controllable gene expression units on surfaces. This localized product enrichment, free of physical boundaries, opens up the possibility to switch and cascade biochemical processes that are based on weak interactions between macromolecules and are thus highly affected by solution concentration.

Materials and methods

Experimental methods

Protocols for surface modification, UV photolithography, biotinylation of deprotected surface amines, synthesis of biotinylated DNA radioactively and nonradioactively labeled, streptavidin-DNA conjugation, luciferase assay are all described in the Supporting information and partly by Buxboim *et al* (2007).

Radioactive DNA density quantitation

Surfaces bound with radioactive DNA were thoroughly rinsed, air-dried, and exposed to phosphorous screen (FUJI), which was then scanned by a phosphorimager (FLA-5100, FUJI). Known amounts of radioactive DNA were spotted on the same surface *without washing* to derive the average specific activity of each DNA. The amount of moles of DNA was derived by dividing the radiation in each spot by the specific activity of that DNA.

Parallel RNA and protein synthesis on a chip in the extract

Daisy-coated silicon dioxide substrates (18 × 18 mm^2) were placed in a custom-made Teflon reaction chamber (details in Buxboim *et al*, 2007) with nine separated regions each containing 10 μl of cell-free reaction mix. Cell-free coupled transcription/translation reactions were carried out using the RTS100 Cell-Free *E. coli* Extract System (Roche) according to the manufacturer protocol. This extract is optimized with minimal nuclease activity and is hence suitable for the use of linear DNA templates. Aliquots were taken from each region on the chip to measure luciferase luminescence. Transcription rates were measured by supplementing the cell-free *E. coli* extract with 0.2 μM ^{32}P-α-rUTP. The reaction was stopped by the addition of 0.2% SDS/20 mM EDTA final concentrations and placed immediately on ice. A total of 1 μl of this stopped reaction was spotted on a polyethyleneimine (PEI) cellulose thin layer chromatography (TLC) plate (Merck). The RNA was resolved from its precursor nucleotides by developing in 0.3 M potassium phosphate, pH=7.0. TLC plates were dried and their radioactive spots were imaged as above. RNA concentration was quantified assuming 0.5 mM endogeneous rNTP.

mRNA synthesis in a minimal transcription-only reaction

A transcription-only reaction was constructed by mixing 5 × transcription buffer (Promega) with 10 mM DTT (Promega), rNTP mix (0.5 mM rATP, rGTP, and rCTP and 0.25 mM rUTP), 3 U μl^{-1} recombinant RNasin ribonuclease inhibitor (Promega), and 2–20 U μl^{-1} T7 RNAP. mRNA production was measured by supplementing the reaction with 0.2 μM ^{32}P-α-rUTP. The reaction was stopped and processed as described above.

RNA degradation rate

Radioactive-labeled luciferase RNA was transcribed from grafted genes using 3 U μl^{-1} t7-RNA polymerase (Roche) in 1 × transcription buffer (Roche) supplemented with 200 μM of rNTPs (each of the four) and 0.2 μM ^{32}P-α-rUTP. The reaction was incubated at 30°C for 200 min. A 5 μl aliquot (2 pmol) was removed from the chip into 20 μl *E. coli* cell extract and further incubated at 30°C. After 2, 5, 15, 40, and 200 min, 3 μl samples were collected, stopped, and quantified as described above.

The theoretical methods for solving the reaction-diffusion equations for transcription/translation are described in the Supporting information.

Supplementary information

Supplementary information is available at the *Molecular Systems Biology* website (www.nature.com/msb).

Acknowledgements

We would like to thank S Safran and T Tlusty for useful discussions. This work was supported by grants from the Israel Science Foundation and the Minerva Foundation.

References

Buxboim A, Bar-Dagan M, Frydman V, Zbaida D, Morpurgo M, Bar-Ziv R (2007) A single-step photolithographic interface for cell-free gene expression and active biochips. *Small* **3:** 500–510

Daube SS, Arad T, Bar-Ziv R (2007) Cell-free co-synthesis of protein nanoassemblies: tubes, rings, and doughnuts. *Nano Lett* **7:** 638–641

Dittmer WU, Kempter S, Radler JO, Simmel FC (2005) Using gene regulation to program DNA-based molecular devices. *Small* **1:** 709–712

Dittmer WU, Simmel FC (2004) Transcriptional control of DNA-based nanomachines. *Nano Lett* **4:** 689–691

Doktycz MJ, Simpson ML (2007) Nano-enabled synthetic biology. *Mol Syst Biol* **3:** 125

Forster AC, Church GM (2006) Towards synthesis of a minimal cell. *Mol Syst Biol* **2:** 45

Isaacs FJ, Dwyer DJ, Collins JJ (2006) RNA synthetic biology. *Nat Biotechnol* **24:** 545–554

Isalan M, Lemerle C, Serrano L (2005) Engineering gene networks to emulate *Drosophila* embryonic pattern formation. *Plos Biol* **3:** 488–496

Ishikawa K, Sato K, Shima Y, Urabe I, Yomo T (2004) Expression of a cascading genetic network within liposomes. *FEBS Lett* **576:** 387–390

Kim J, White KS, Winfree E (2006) Construction of an *in vitro* bistable circuit from synthetic transcriptional switches. *Mol Syst Biol* **2:** 68

Luisi PL, Ferri F, Stano P (2006) Approaches to semi-synthetic minimal cells: a review. *Naturwissenschaften* **93:** 1–13

Milner ST (1991) Polymer brushes. *Science* **251:** 905–914

Murtas G, Kuruma Y, Bianchini P, Diaspro A, Luisi PL (2007) Protein synthesis in liposomes with a minimal set of enzymes. *Biochem Biophys Res Commun* **363:** 12–17

Noireaux V, Bar-Ziv R, Godefroy J, Salman H, Libchaber A (2005) Toward an artificial cell based on gene expression in vesicles. *Phys Biol* **2:** P1–P8

Noireaux V, Bar-Ziv R, Libchaber A (2003) Principles of cell-free genetic circuit assembly. *Proc Nat Acad Sci USA* **100:** 12672–12677

Noireaux V, Libchaber A (2004) A vesicle bioreactor as a step toward an artificial cell assembly. *Proc Nat Acad Sci USA* **101:** 17669–17674

Nord O, Uhlen M, Nygren PA (2003) Microbead display of proteins by cell-free expression of anchored DNA. *J Biotechnol* **106:** 1–13

Seelig B, Szostak JW (2007) Selection and evolution of enzymes from a partially randomized non-catalytic scaffold. *Nature* **448:** U828–U831

Seeman NC (2005) From genes to machines: DNA nanomechanical devices. *Trends Biochem Sci* **30:** 119–125

Shimizu Y, Inoue A, Tomari Y, Suzuki T, Yokogawa T, Nishikawa K, Ueda T (2001) Cell-free translation reconstituted with purified components. *Nat Biotechnol* **19:** 751–755

Shivashankar GV, Liu S, Libchaber A (2000) Control of the expression of anchored genes using micron scale heater. *Appl Phys Lett* **76:** 3638–3640

Sunami T, Sato K, Matsuura T, Tsukada K, Urabe I, Yomo T (2006) Femtoliter compartment in liposomes for *in vitro* selection of proteins. *Anal Biochem* **357:** 128–136

Szostak JW, Bartel DP, Luisi PL (2001) Synthesizing life. *Nature* **409:** 387–390

Tawfik DS, Griffiths AD (1998) Man-made cell-like compartments for molecular evolution. *Nat Biotechnol* **16:** 652–656

Valle F, Favre M, De Los Rios P, Rosa A, Dietler G (2005) Scaling exponents and probability distributions of DNA end-to-end distance. *Phys Rev Lett* **95:** 158105